JOURNAL OF CATALYSIS **114**, 121–135 (1988)

Cracking of *n*-Decane on Zeolite Catalysts: Enhancement of Light Hydrocarbon Formation by the Zeolite Field Gradient

C. MIRODATOS AND D. BARTHOMEUF*

*Institut de Recherches sur la Catalyse, Laboratoire Propre du CNRS Conventionné à l'Université Claude Bernard Lyon I, 2 Avenue Albert Einstein, 69626 Villeurbanne Cédex, and *Laboratoire de Réactivité de Surface et Structure, UA 1106, CNRS, Université Paris VI, 4 Place Jussieu, 75252 Paris Cédex 05, France*

Received November 10, 1986; revised February 19, 1988

The selectivity in the cracking of *n*-decane and, more generally, *n*-alkanes in zeolites ZSM-5, erionite, offretite, mordenite, and faujasite is characterized by the ratios C_2/C_4 and C_3/C_4, independent of the olefinic or branched character of the products. It is proposed that when high ratios are observed, the nonclassical cracking mechanism through pentacoordinated carbonium ion (PCI) prevails over the classical β-scission mechanism. Low values would characterize the reverse trend. The PCI pathway is associated with the presence of high field gradients arising from at least one of three parameters: highly constraining porosity (small pores and/or tortuosity); low charge density (low Al content, i.e., low density of positive charges, namely protons and metal cations); and polarizing cations. The field gradient selectivity does not depend on the acid strength itself, nor straightforwardly on the pore volume left free after coke deposition. It is proposed that the ratios C_2/C_4 and C_3/C_4 be considered field gradient selectivity indexes.

INTRODUCTION

The high activity of zeolites was early recognized as being related to the polarization of molecules in cages (*1, 2*). Later, the great interest in shape-selective catalysis demonstrated the importance of steric factors which direct the selectivity very specifically (*3*). In recent years it has been shown that besides the purely geometric effects of this shape selectivity, the zeolite topology and structure may induce changes in properties related to framework or cage energetic parameters. It was shown that shifts of the AlK_β X-ray emission band energies of several zeolites can be separated into three groups based either on framework structure type or on framework density. The first group includes A, X, Y, and Rho (cubooctahedra); the second, offretite and erionite (cancrinite units); and the third, mordenite (crosslinked five-ring chains) (*4*). A cage effect was also evidenced for the chemical shift in ^{13}C NMR spectra of tetramethylammonium ions in zeolites (*5*) and in ^{129}Xe NMR studies (*6*). The values depend on the type of cage in which the organic ion or the Xe atom is trapped. Altogether, AlK_β, ^{13}C, and ^{129}Xe results suggest that for a given cage type there would be associated a specific energy of framework atoms and of atoms of adsorbed species. This may imply a particular crystal field.

In the study of adsorption of molecules in zeolites it is usual to consider the contribution to the energy of adsorption of the terms due to field–dipole and field–quadrupole interactions. The dipole (*1, 2*) and quadrupole behaviors of molecules are eventually induced in the zeolite on polarization of the adsorbates in the cages. Since the field and field gradient should exist in any zeolite as soon as charges are present it seems reasonable to consider that such interactions, when present, will affect molecules in cavities.

Previous results of *n*-alkane cracking in erionite and offretite showed a selectivity dependence on the cage structure not related to any geometric effect (*7*). Further catalytic experiments in a large variety of zeolites confirmed these findings and were

0021-9517/88 $3.00

explained on the basis of the dependence of selectivity in catalysis on the homogeneity or heterogeneity of the energetic environment surrounding the reacting molecules (*8*). Such an assumption requires that introducing a high asymmetry in the charge distribution on the cage walls should affect the crystal field gradient and then the selectivity. In this line the present paper reports the influence of Al framework content and of polyvalent cations on the selectivity in the cracking of *n*-decane. This alkane was chosen to avoid any constraint due to a very short length of molecule. A linear alkane is preferred over branched ones to limit shape-selectivity effects.

EXPERIMENTAL

Materials

The various zeolites used are listed in Table 1 with their Si/Al ratio and extent percentage of cation exchange for protons. Sample 1 is a HNaX in which 41% of Na^+ have been exchanged with NH_4^+ of an ammonium acetate solution. Materials 2 to 4 are HNaY progressively exchanged for protons. Among the three dealuminated Y zeolites (5–7), $\text{HNaY}_{\text{D-4.5}}$ refers to a material treated with EDTA (*9*), and $\text{HNaY}_{\text{D-7}}$ refers to a material treated with ammonium hexafluorosilicate (*10*). Sample LZY-82 is the commercial Linde zeolite. Its framework Si/Al ratio determined from unit cell (u.c.) parameters is the same as that for $\text{HNaY}_{\text{D-4.5}}$. A HNaY was exchanged with $MgCl_2$ or with $LaCl_3$ giving samples 8 and 9 containing, respectively (8.1 Na + 29.4 eq Mg/u.c.) and 5 Na + 30 eq La/u.c.), referred to as HNaMgY and HNaLaY. A ZSM-5 zeolite $Na_{0.2}H_{2.65}$ $(AlO_2)_{2.85}$ $(SiO_2)_{93.15}$ and an erionite from Société Chimique de la Grande Paroisse $Na_{2.5}K_{4.7}H_{0.4}(AlO_2)_{7.6}(SiO_2)_{24.4}$ are referred to as samples 10 and 11 (*8*). Sample 12 is an of-

TABLE 1

Activity and Selectivity in the Cracking of *n*-Decane at 793 K

Zeolite	Si/Al	Cation exchange for proton (%)	Activity (molecules s^{-1} g^{-1}) × 10^{-15}	C_2/C_4	C_3/C_4
1. HNaX-41	1.2	41	2[a]	0.19	1.03
2. HNaY-41	2.4	41	43	0.32	1.33
3. HNaY-67	2.4	67	104	0.18	1.07
4. HNaY-87	2.4	87	347	0.23	1.32
5. $\text{HNaY}_{\text{D-4.5}}$	4.5	84	390	0.52	2.22
6. LZY-82	4.5[b]	98	2600	0.50	2.23
7. $\text{HNaY}_{\text{D-7}}$	7	83	541	0.77	2.86
8. HNaMgY	2.4	33	347	0.44	2.00
9. HNaLaY	2.4	37	650	0.28	1.76
10. ZSM-5	33	95	867	1.14	3.10
11. Erionite	3.2	78	390	0.94	2.29
12. HKMg-OFF	4	52	498	0.51	1.79
13. HK-OFF-76	4	76	1892	0.45	1.68
14. HK-OFF-70	4	70	455	0.40	1.58
15. HK-OFF-38	4	38	390	0.23	1.27
16. HK-OFF-11	4	11	<1[a]	Not available	
17. H-MOR[c]	5	94	130	0.45	1.39

[a] For samples 1 and 16, values corrected for thermal cracking (low conversion).

[b] Framework unit cell deduced from unit cell parameter.

[c] Steamed sample.

fretite partly exchanged with Mg containing 0.83 K^+ and 0.86 eq Mg^{2+}/u.c. A series of variously exchanged offretites (13–16) prepared from a sample provided by Barrer and Harding (*11*) contain protons and, respectively, 0.84, 1.03, 2.16, and 2.75 K^+/u.c. (8). A steamed mordenite $Na_{0.47}H_{7.53}(AlO_2)_8(SiO_2)_{40}$ is material 17.

n-Decane Cracking

Catalytic experiments were performed in a conventional dynamic microreactor connected to an automated system of gas chromatographic sampling and analysis. *n*-Decane cracking was carried out in flowing hydrogen under the following experimental conditions: flow rate 1.8–2.4 liters/h, reaction temperature 753–793 K, partial pressure ratio $P_{H_2}/P_{C_{10}H_{22}} = 75$.

The actual conversion level was limited to about 10% by adjusting the weight of catalyst to avoid any diffusion effect in the catalytic bed. Catalytic activity is expressed as molecules of *n*-decane converted per second and per gram of catalyst. For the case of poorly active material, the reaction rate is corrected for the conversion emanating from purely thermal cracking. The activity values given in the paper are those obtained when the selectivity ratios C_3/C_4 or C_2/C_4 are nearly constant, i.e., after 2–3 h on-stream unless otherwise specified.

RESULTS AND DISCUSSION

Catalytic activity values are given in Table 1 for the materials tested. The purpose of the work is to consider parameters affecting the selectivity, so the Results and Discussion will focus on product distributions. Comments on their relation with catalytic activity will be made when necessary.

Product Distribution

It was observed in the cracking of light alkanes (*n*-C_7 and *n*-C_8) that acidic zeolites with different structures could be ranked according to their ability to produce large (or small) amounts of C_1, C_2, and C_3 and simultaneously small (or large) amounts of C_4 and heavier hydrocarbons when iso + normal and unsaturated + saturated are considered altogether (*8*). No obvious correlation could be obtained when reaction products were classified according to their branching or saturation degree.

The cracking of *n*-decane gives mainly C_1 to C_6 products. In all cases C_1 yields are low; moreover they include a significant contribution of thermal cracking. They will not be considered here. The absence of C_7 to C_9 hydrocarbons products is related to a further cracking at 793 K to smaller fragments. Figure 1 shows an example of product distribution with faujasite and offretite

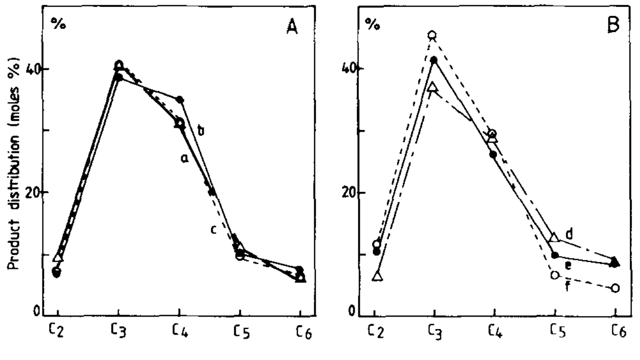

FIG. 1. Product distribution in the cracking of *n*-decane at 793 K for various cation-exchanged HNaY (A) and HK-OFF (B). Cation exchange percentage for HNaY: a = 41, b = 67, c = 87; for HK-OFF: d = 38, e = 70, f = 76.

TABLE 2

Influence of Percentage Conversion on Selectivity[a]

Zeolite	Weight (mg)	Conversion (%)	Average activity (molecules s^{-1} g^{-1}) × 10^{-15}	C_3/C_4	C_2/C_4
Change with contact time					
HNaX-41	84.0	0.1		1.05	0.19
	113.1	0.2	2[b]	0.97	0.18
	217.3	0.3		1.07	0.19
HNaY-67	40.5	1.9	102[b]	1.11	0.20
	76.2	3.7		1.07	0.18
$\text{HNaY}_{\text{D-7}}$	84.2	21.2	541	2.86	0.77
HNaMgY	73.1	11.6	347	2.00	0.44
Change with time on stream					
HNaY-67	76.2				
After 0.3 h		4.9	137	1.10	0.20
0.75 h		4.5	126	1.07	0.18
3 h		3.7	104	1.07	0.18
17 h		3.5	98	1.00	0.17
$\text{HNaY}_{\text{D-7}}$	84.2				
After 3 h		21.2	541	2.86	0.77
26 h		18.2	462	2.66	0.72
HK-OFF-76	11.4				
After 2 h		10.1	1892	1.68	0.45
3 h		9.0	1689	1.66	0.42

[a] Carrier gas flow 2.4 liters h^{-1}, t = 793 K.

[b] Average value for all experiments on those catalysts.

of various cation content. The shapes of the curves for product distribution differ greatly from sample to sample. The general trend is that, as already observed for n-C_7 and n-C_8 cracking, a decrease in C_4 and heavier products is accompanied by an increase not only in C_3 but also in C_2 formation. The parallel production of C_2 and C_3 on one side and of heavier hydrocarbons on the other suggests consideration of the formation of products through ratios of light to heavier hydrocarbons. Typically, C_2/C_4 or C_3/C_4 ratios vary similarly and significantly when moving from one zeolite to another and therefore will be considered as selectivity indexes in the present paper. Ratios C_2/C_5, C_3/C_5, C_2/C_6, and C_3/C_6 have the same behavior as those indexes.

Effect of Conversion Level

The very large range of activities for the catalysts tested did not allow us to use the same sample weight. As stated under Experimental the conversion was maintained below 10%. Since it is well known that the selectivity in many cracking reactions (for instance the ratios iso/n or alkenes/alkanes) depends on the extent of conversion, it was important to check any change in the ratios C_3/C_4 or C_2/C_4 with the conversion percentage. Table 2 reports some values obtained for the same carrier gas flow (2.4 liters h^{-1}) and various sample weights. For a given zeolite, HNaX-41 or HNaY-67, the two- to almost threefold change in sample weight increases proportionally the conversion but does not affect significantly the C_2/C_4 and C_3/C_4 ratios. This shows that the results obtained for the X and Y zeolites are not disturbed by external diffusion effects. Nearly similar sample weights (i.e., in the range 73–84 mg) give for different zeolites different extents of conversion, ca. 0.1 to 21%, and also different C_2/C_4 and C_3/C_4 values. The absence of a unique and direct correlation between selectivity and percentage conversion is also confirmed on observation of catalyst aging. For HNaY-67, $HNaY_{D-7}$, and HK-OFF-76 zeolites (Table 2) the decrease in catalytic activity with time on-stream is not related to a significant change in C_2/C_4 and C_3/C_4 ratios.

Tables 1 and 2 suggest that for a large variety of zeolites there is no obvious correlation between selectivity ratios C_2/C_4 and C_3/C_4 in *n*-decane cracking and extent of conversion. It was already observed that neither aging nor percentage conversion parallels the C_2, C_3, C_4 product distribution in *n*-C_7 and *n*-C_8 cracking for different zeolites (*8*). One may wonder whether the formation of light products could arise specifically in the zeolites with the smaller pores, due to faster diffusion (see pore size in Table 3). This point was studied in great detail in the cracking of *n*-C_7 and *n*-C_8 by changing the pore size by coke deposition under various conditions. No correlation was found with the C_2/C_4 or C_3/C_4 ratios, even in ZSM-5, whereas in shape-selective reactions governed by diffusion phenomena the coke deposition drastically changed the selectivity (*8*). In the present case zeolites have also been studied as a function of time on-stream as described in Table 2 for three samples. The aging due to coke deposition which restricts the pore size does not increase the formation of C_2 and C_3, but a small decrease is observed in all cases (Table 2). This discards any explanation based on a favored diffusion of light hydrocarbons.

Effect of Acid Strength

Increasing the acid strength makes feasible the cracking of stable molecules like *n*-alkanes. The effect on product distribution, alkenes or alkanes, branched or not, is not perfectly understood. The possibility then arises of a change in C_2/C_4 and C_3/C_4 ratios with acid strength. The latter parameter can be modified in several ways: (i) increase in Si/Al ratio by dealumination, (ii) progressive exchange of metal cations by protons (increase in the density of protons), (iii) use of different zeolite types. In dealumination, there is a simultaneous decrease in the density of positive charges (protons plus metal cations) and in the density of protons. To vary selectively one parameter at a time, for instance the density of protons in a first step, the acid strength is changed as in (ii) by partial replacement of cations with protons: Fig. 1 reports the distribution of products, and Figure 2, the ratios C_2/C_4 and C_3/C_4 when the cation Na^+ or K^+ is replaced by protons in the series HNaY or HK-OFF and erionite, respectively. No value is

TABLE 3

Selectivity Ratios C_2/C_4 and C_3/C_4 in the Cracking of *n*-Alkanes and Pore System, and Acid Strength of Zeolites

Zeolite	Pore type	Cage size (nm)	Aperture (nm)	C_3/C_4			C_2/C_4			Acid strength[b] (*K*)
				n-C_7[a]	*n*-C_8[a]	*n*-C_{10}	*n*-C_7[a]	*n*-C_8[a]	*n*-C_{10}	
ZSM-5	Channel		0.54 × 0.56	1.22	1.1	3.1	0.30	0.54	1.14	
	Channel intersection	0.9	0.52 × 0.58							
Erionite	Cage	1.3 × 0.63		1.7	1.2	2.3	0.33	0.28	0.94	
H-OFF	Gmelinite + channel	0.65 × 0.78	0.36 × 0.52 0.63	0.96	0.77	1.68	0.08	0.17	0.45	675
HK-OFF	Channel		0.63	0.83	0.45	1.27	0.10	0.06	0.23	
Mordenite	Channel		0.67 × 0.7	0.86	0.43	1.39	0.06	0.09	0.45	725
HNaY	Supercage	1 to 1.3	0.74	0.8	0.48	1.3	0.06	0.06	0.23	625
HNaX	Supercage	1 to 1.3	0.74			1.03		0.04	0.19	

[a] Cracking reaction at 723 K (*8*).

[b] Expressed as maximum temperature of pyridine adsorption on Brønsted sites.

given for C_2/C_4 ratio of the weakly exchanged offretite or for its product distribution. It was confirmed on the basis of blank experiments that in addition to C_1 and C_2 products of the proper zeolitic reaction, small amounts of C_1 and C_2 were produced from thermal cracking (including possibly the inner surface of the reactor). For very unactive samples, like the highly cationated materials, this thermal cracking predominates, making the C_2/C_4 ratio determination meaningless.

Within experimental error, the results presented in Figs. 1 and 2 show that there is no significant change for the Y and erionite series either in the product distribution, evaluated from the carbon number, or consequently in selectivity ratios C_2/C_4 and C_3/C_4. It is well accepted that in cracking reactions acid strength is a major parameter that directs the catalytic activity and the ratios of linear/branched hydrocarbons and alkenes/alkanes. It is also well established that the density of protons and the strength of acidity increase for zeolites (particularly Y type) at exchange levels in the range 50–100%. Nevertheless, Fig. 2 shows that at least for three highly exchanged samples (two Y and one erionite) the C_2/C_4 and C_3/C_4 ratios do not depend on a high exchange level, i.e., on acid strength. This suggests that the cracking pattern giving C_2 and C_3 is not directed by acid strength. It is worthwhile noting that the two zeolite structures, Y and erionite, which show constant C_2/C_4 and C_3/C_4 values in the cracking of *n*-C_7 and *n*-C_{10} (Fig. 2), have a pore system which is identical at any cation content, i.e., the molecules always undergo the same structure influence.

By contrast, the formation of light products increases for the offretite series as the metal content decreases, i.e., when strong acidity develops, as shown in Ref. (*7*). This might suggest for this case a correlation between acid strength and selectivity. In fact, reference to previous works concerning the cracking of *n*-heptane and *n*-octane in offretite and erionite catalysts (*7*, *8*) reveals that offretite displays a unique behavior which suggests that changes in product distribution be correlated not to acid strength but to cage accessibility monitored by the cation content. In low-cation-exchanged offretite, the molecules move only along the channels. At a high exchange level they can also enter the smaller gmelinite cages where they move closer to the walls, i.e., in a much more heterogeneous field which could favor a different cracking mode. The changes in selectivity ratios C_2/C_4 and C_3/C_4 occurred abruptly between 33 and 45% cation exchange for protons, a level at which the gmelinite cavity starts to be accessible to the reacting molecules. Therefore, as for the C_7–C_8 *n*-alkanes, the increase in C_2/C_4 and C_3/C_4 ratios observed with *n*-decane in the present work as the

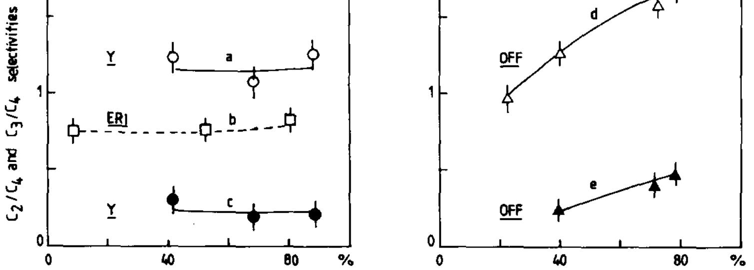

FIG. 2. Change in selectivity ratios C_3/C_4 (a, b, d) and C_2/C_4 (c, e) for HNaY (a, c), HK-OFF (d, e), and erionite (b) as a function of ion exchange for protons in the cracking of *n*-decane at 793 K (HNaY and HK-OFF) and of *n*-heptane at 723 K (erionite).

TABLE 4

Estimation of Field Gradient From Ref. (*16*)

Zeolite	Average field F at indicated distance from S_{II} cation surface (V nm^{-1})			Average ΔF per nm between indicated distances from S_{II} cation surface (V nm^{-2})	
	0.100[a]	0.175	0.250	$[\Delta F/0.075]_{0.100}^{0.175}$	$[\Delta F/0.075]_{0.175}^{0.250}$
NaX	0.194	0.064	0.036	−1.73	−0.37
NaY	0.257	0.106	0.053	−2.01	−0.71
MgY	0.936	0.418	0.223	−6.91	−2.60

[a] Distance in nm.

cations are replaced by protons is also probably a consequence of a different cracking mechanism in the small gmelinite cages. Nevertheless, it must also be considered that a small dealumination of offretite might occur during ion exchange, as suggested by the shift in IR wavenumber of T–O bonds (*12*). A rise in Si/Al ratio may increase the C_2/C_4 and C_3/C_4 ratios as it does for Y zeolite (*13–15*). As will be seen later, these selectivity changes are also explained by the existence of two superimposed cracking mechanisms.

Table 3 reports an example of changes in acid strength as in (iii) by considering the different zeolites—HY, offretite, H-mordenite. The acid strength determined in previous infrared studies is expressed as the limit temperature of pyridinium ion stability. It increases from Y to offretite and mordenite. The C_3/C_4 selectivity ratio for *n*-heptane, *n*-octane, isooctane (*8*), and *n*-decane is the highest in any case for H-offretite which displays intermediate acid strength. The results again tend to show that acid strength is not the main parameter on which the relative production of light and heavy hydrocarbons depends.

Field Gradient

It was previously proposed that *n*-C_7 and *n*-C_8 cracking selectivity is related to homogeneity or heterogeneity of the energetic environment in the cages (*8*). This latter factor can be reasonably estimated through the field gradient in the cavities. The field gradient depends on the distribution of charges, positive and negative, in the space surrounding the moving molecules.

An evaluation of the field and field gradient tensor for all the zeolites considered here is not presently available in the literature. Field calculations for faujasites have been performed (*2, 16*). The electrostatic field is expressed as F = grad ϕ, with $\phi_j = \Sigma_{ik}\, q_{ik}/r_{ikj}$ at point j, where q_{ik} is the charge at ion i at lattice point k at distance r_{ikj} from the potential point j. The field gradient tensor involves the second derivative of ϕ: $\delta^2\phi/\delta x^2$, $\delta^2\phi/\delta x \delta y$. Table 4 reports values obtained for the fields at 0.1, 0.175, and 0.250 nm from the surface of cations located in S_{II} sites (*16*). The difference in field ΔF per nanometer between these values can be considered as an estimate of the field gradient. The calculation does not take into account the changes in field and consequently in field gradient that are expected if various cation types are simultaneously distributed in the sites of the same material and if the polyvalent cations bear hydroxyls. They can nevertheless be considered as a guideline in faujasite, probably also valid if protons are considered instead of cations. It is seen that ΔF per nanometer is higher at the lower Al content of NaY compared with NaX. It can be inferred that for the same faujasite structure, the ΔF per nanometer value should be even higher at a lower Al level, giving rise to more heterogeneous

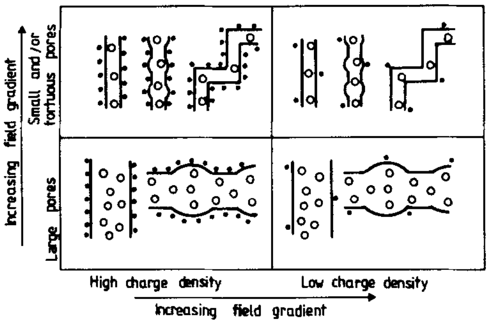

FIG. 3. Relationship between the changes in field gradient and both the changes in charge density (or Al content) and in pore size and tortuosity. (o, molecules in pores; •, Al atoms).

fields in the cage volume. The calculation also shows that ΔF per nanometer is larger for the highly polarizing Mg^{2+} ion, as one might expect. It further suggests that the closer from the walls (i.e., from the charges) the molecules are, the more heterogeneous are the fields they undergo since ΔF per nanometer is quite high close to the surface. This means that the smaller or the more tortuous the cages are, the higher are the field gradients to consider. From those three effects on the field gradient (Al content, pore geometry, polarizing cation) the first and the second one are tentatively outlined in Fig. 3. The bottom left part corresponds to zeolites with large cages or channels and high Al content where the molecules move in a space with rather homogeneous fields. For zeolites with smaller pores or lower Al content, the field and field gradient increase, the ultimate case being represented in the upper right part of Fig. 3. These three parameters will be considered in greater detail in the following sections.

Effect of Charge Density in Faujasites

It is well known that raising the Si/Al ratio in zeolites increases the acid strength. Simultaneously, the density of charges decreases. The results in Figs. 1 and 2 and Table 3 showed that C_2/C_4 and C_3/C_4 selectivities are not intrinsically related to acid strength. Any change in these ratios with

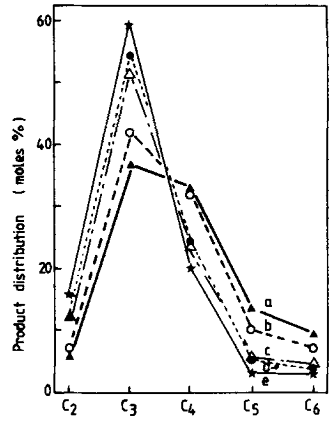

FIG. 4. Product distribution in the cracking of n-decane at 793 K for protonic faujasite of different Al content. Si/Al values: (a) 1.2, (b) 2.4, (c) 4.5, (d) 4.5 (framework), (e) 7.

Si/Al values could therefore be related only to the charge density. The product distributions obtained in the n-decane cracking for various Al contents in faujasites are given in Fig. 4. Figure 5 reports the resulting changes in selectivities C_3/C_4 and C_2/C_4 as a function of Al content. Boh figures clearly show the reverse trend for a higher production of light hydrocarbons (C_2–C_3) on the one side and for a lower production of heavier hydrocarbons (C_4^+) on the other when the Si/Al ratio increases. In contrast, as seen in Table 5, no drastic changes are observed in the inner distribution (i.e., linear to branched or saturated to unsaturated

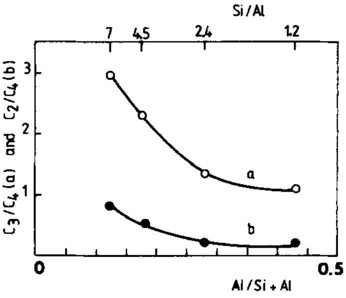

FIG. 5. Dependence of selectivities C_3/C_4 (a) and C_2/C_4 (b) on the Al content of faujasites (n-decane cracking at 793 K).

TABLE 5

Detailed Distribution of C_3/C_4 Products in the *n*-Decane Cracking at 793 K

Zeolite[a]	$\frac{C_3}{\Sigma C_3}$	$\frac{C_3^=}{\Sigma C_3}$	$\frac{i\text{-}C_4}{\Sigma C_4}$	$\frac{n\text{-}C_4}{\Sigma C_4}$	$\frac{IC_4^=}{\Sigma C_4}$	$\frac{i\text{-}C_4^=}{\Sigma C_4}$	$\frac{c.C_4^=}{\Sigma C_4}$	$\frac{t.C_4^=}{\Sigma C_4}$	$\frac{\Sigma C_4^=}{\Sigma C_4}$	$\frac{i\text{-}C_4 + i\text{-}C_4^=}{\Sigma C_4}$	C_3/C_4
	× 100					× 100					
2. HNaY-41	14	86	3	14	13	22	21	26	83	25	1.33
3. HNaY-67	10	90	8	13	13	22	16	27	79	30	1.27
4. HNaY-87	9	91	9	11	10	18	17	35	80	27	1.32
5. $HNaY_{D\text{-}4.5}$	15	85	11	19	10	21	17	21	70	32	2.22
6. LZY-82	14	86	19	16	9	17	14	25	65	36	2.23
7. $HNaY_{D\text{-}7}$	17	83	27	22	6	14	11	19	51	41	2.86
8. HNaMgY-33	13	87	15	15	9	19	15	27	70	34	2.00
9. HNaLaY-37	11	89	5	13	10	23	21	28	82	28	1.76
10. ZSM-5	14	86	9	26	7	21	20	16	65	30	3.1
11. ERIONITE	8	92	0	18	22	0	33	28	82	30	2.3
12. HKMg-OFF	8	92	14	10	11	21	16	27	76	35	1.8
13. HK-OFF-76	7	93	9	9	12	21	20	29	82	30	1.68
14. HK-OFF-70	7	93	11	8	11	21	17	31	81	32	1.58
15. HK-OFF-38	7	93	6	6	12	26	19	30	88	32	1.27
17. H-MOR	12	88	1	16	14	27	22	20	83	28	1.39

[a] Due to low conversion values are not available for HNaX and HK-OFF-11.

ratios) of the C_2, C_3, and C_4 products throughout the series of catalysts studied. Let us note only a trend to a lower production of alkenes for the more dealuminated samples. For example, the proportion of olefinic C_4 decreases from 80 to 51% when the Si/Al ratio increases from 2.4 to 7. This alkene consumption could arise from formation of coke or coke precursors through H transfer, as was observed for the change with time on-stream of the production of propene and propane in *n*-heptane cracking (*8*). Hydrogen transfer which is a bimolecular reaction requires close acid sites. It is known that a decrease in this reaction is observed only at high Si/Al ratios, when AlO_4 tetrahedra are isolated (*17*). The dealuminated materials studied here have too low a Si/Al ratio to expect any hydrogen transfer decrease.

The EDTA-extracted Y ($HNaY_{D\text{-}4.5}$) (curve c, Fig. 4) and LZY-82 zeolite (curve d, Fig. 4) give very similar selectivities. They have the same framework Al content, the LZY-82 zeolite containing extra-framework species. This last sample gives the highest reaction rate, six times more than that for the $HNaY_{D\text{-}4.5}$ material (Table 1). This very probably arises from the presence of extra-framework deposits which may change the strength as in mordenite (*18*). From the similar selectivities observed for both samples it is inferred that extra-framework aluminum does not significantly modify the distribution of products according to their carbon number. This again shows that changes in acid strength do not necessarily induce changes in light and heavy product distribution. Thus, the important parameter seems to be framework Al content which directs the density of charges in the materials; the observed increase (up to three times) in the ratios C_3/C_4 and C_2/C_4 with decreasing Al content (Fig. 5) is in line with the expected rise in field gradient as the average distance between charges increases, i.e., when the number of AlO_4^- tetrahedra decreases.

Effect of Cation

The field gradient is dependent on the polarizing power of the cation. It should also

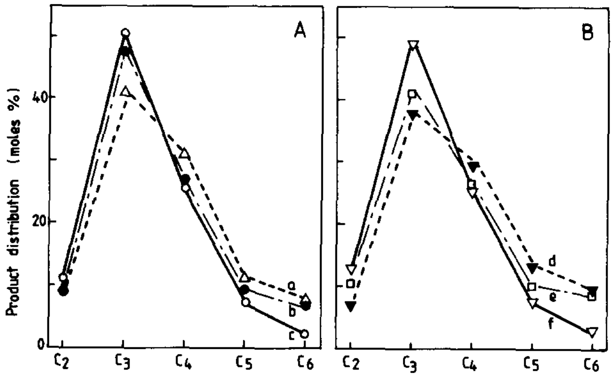

FIG. 6. Product distribution in the cracking of *n*-decane at 793 K for (A) faujasites (a, HNaY-41; b, HNaLaY; c, HNaMgY) and (B) offretite (d, HK-OFF-38; e, HK-OFF-70; f, HKMg-OFF).

be more important when the distance between positively charged atoms (metal cation and proton) increases. This occurs when polyvalent cations are present since their number decreases as charge increases. For Na^+ and K^+ the polarizing power expressed as Ze/r^2 in arbitrary units is, respectively, 1.1 and 0.57. It increases to 4.74 for Mg^{2+} and 2.27 for La^{3+}. The total number of atoms with a positive charge in faujasite is 56 for HNaY, 22.8 for HNaMgY (sample 8), and 15 for HNaLaY (sample 9). Moreover, Mg^{2+} and La^{3+} are preferentially located in the sodalite cage, which decreases even more the number of positively charged atoms accessible to hydrocarbons in the supercage.

The effect of polyvalent cations (Mg^{2+} and La^{3+}) in faujasite and offretite on the product distribution is depicted in Figs. 6A and B. Higher production of C_2 and C_3 and lower production of C_4^+ hydrocarbons are noted when Mg^{2+} or La^{3+} replaces monovalent ions. For faujasites, samples 2, 8, and 9 in Fig. 6A have a similar degree of cation exchange. The selectivity ratios C_2/C_4 and C_3/C_4 given in Table 1 reflect this influence of cation valence. It was stated earlier that those ratios do not depend, in faujasite, on Na^+ content which has a rather low polarizing power. Similar behavior was already observed for erionite at any K^+ level (*8*). Replacement of protons with Mg^{2+} ions gives higher C_2/C_4 and C_3/C_4 values; La^{3+} cations increase mainly the C_3/C_4 ratio. This is in line with the expected increase in field gradient due to polyvalent cations.

Concerning the inner distribution of each hydrocarbon group (Table 5), the effect of the polarizing cation (especially magnesium) is similar to that of the dealumination, i.e., a slight decrease in alkene production with regard to the saturated products. For example, the proportion of alkene in the C_4 group decreases from 80 to 70% and from 81–88 to 76% when magnesium is added to faujasite and offretite, respectively. The changes in alkene/alkane ratios with dealumination or the presence of polarizing cations appear to be independent of the changes in the C_3/C_4 and C_2/C_4 ratios.

Effect of Cages

It is worthwhile noting in Table 1 that the C_2/C_4 and C_3/C_4 selectivity ratios may vary from one given zeolite structure to another, even for a similar Si/Al ratio. This is in line with the influence of the cage on energy heterogeneity proposed for n-C_7 and n-C_8 cracking and this influence may become the leading parameter for zeolites with small cages (*8*). The distribution of products for the zeolites not yet described in the previous sections shows in Fig. 7 that, as for n-C_7 and n-C_8 cracking, C_2 and C_3 production

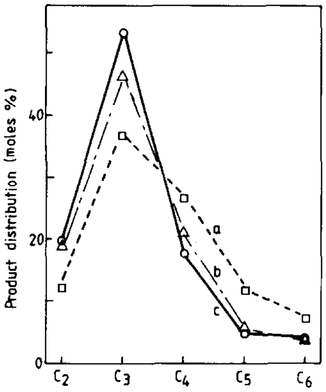

FIG. 7. Product distribution in the cracking of n-decane at 793 K for (a) mordenite, (b) erionite, and (c) ZSM-5.

varies in a direction opposite that for C_4 and heavier hydrocarbons. The smaller or the more tortuous the cages, the higher is the production of light hydrocarbons. Table 3 shows that the highest proportion of light hydrocarbons is obtained with ZSM-5 in C_{10} cracking, whereas this is achieved with erionite in C_7–C_8 cracking. The behavior of erionite could be related to the known "window effect" (*19*), by which C_7 and C_8 molecules are specifically trapped in the erionite cages, possibly favoring a higher proportion of C_2 and C_3. The alkene/alkane and iso/n ratios given in Table 5 for n-decane cracking do not allow a general correlation to be made with the zeolite type.

Some results from the literature can be explained on the basis of the same cage effects. Values taken from Ref. (*20*) allow calculation of the C_3/C_4 ratios of products formed in fluid cracking units. They are reported in Table 6 and show a trend parallel to what is described in Table 3. The high activity of the RE-offretite suggests that gmelinite windows are free of cations. This explains its C_3/C_4 selectivity close to that of pure RE-gmelinite. Both are more selective for C_3 formation than Y and X as in the present study of n-decane cracking results.

It was also observed that clinoptilolite and even ferrierite, whose pores are, respectively, 0.44 × 0.72 and 0.43 × 0.55 nm, give very large amounts of C_1 and C_2 in the cracking of a mixture of n-hexane and 3-methylpentane (*21*). Those zeolites are in a range of pore size that should give high gradients and consequently high production of light products.

A more quantitative approach to the influence of cages would be very valuable. Nevertheless, presently too little is known of zeolites to appreciate the field gradient in many zeolite structures, as very often the Si and Al distribution and cation population in the various sites are not known. Moreover, calculations of field gradient should take into account parameters that are not yet understood and that occur during the process of catalysis (displacement of metal cations and of protons, modification of the shape and electronic configuration of molecules in cages). As a consequence, one should be cautious in comparing the field gradient in different structures on the sole basis of Si/Al ratio or cation content.

Effect of Temperature

Cracking has been carried out in the range 750–795 K. Figure 8 shows the general trend for an increase in C_3/C_4 ratio as reaction temperature increases. C_2/C_4 values (not reported here for clarity) increase similarly. The results suggest that a reaction mechanism that would give more light products is favored at high temperatures.

Reaction Mechanism and Field Gradient

The cracking of n-decane (*22*) or n-hexane (*23*) in alkali metal-exchanged zeolites, i.e., materials without protonic acidity, was shown to proceed through the formation of radical species. This gives rise to C_2 as the major product with much C_1 and C_3. Large amounts of α-alkenes but no or small amounts of branched molecules are formed. At variance with this observation, significant amounts of branched isomers, for instance 25–41% in the C_4 cut (Table 5), are obtained in the present study. Moreover, it is well accepted that catalytic

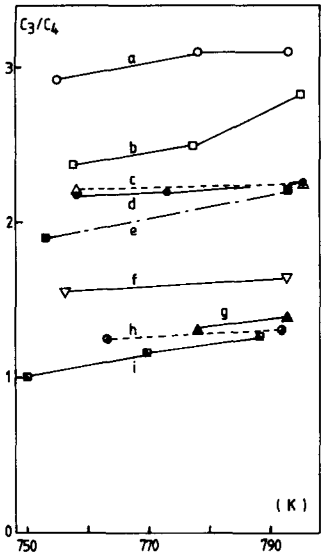

FIG. 8. Changes in C_3/C_4 ratio for *n*-decane cracking as a function of reaction temperature: (a) ZSM-5, (b) $HNaY_{D-7}$, (c) LZY-82, (d) erionite, (e) $HNaY_{D-4.5}$, (f) HK-OFF-76, (g) mordenite, (h) HNaY-41, (i) HK-OFF-38.

cracking prevails in protonic zeolites (*24*). Therefore the contribution of a radical mechanism is not considered here.

The classical reaction mechanism in catalytic cracking involves several steps. Competition between β-scission, bimolecular hydrogen transfer, isomerization, and buildup reactions leads to a large variety of products (*25*). Hydrogen transfer has been proposed to account for the changes in C_4 alkene/alkane ratio with Al content at high Si/Al ratios and with the presence of polarizing cations. Isomerization is effective for the formation of branched products. As far as the formation of light products is concerned, independently of their olefinic or branched character, β-scission is the only step that involves the splitting of a C–C bond. According to the rules of stability of carbenium ions, formation of C_1 and C_2 is not favored through this mechanism. The major products are C_3–C_6 hydrocarbons. A more recent mechanism deduced from comparison with superacids in solutions (*26, 27*) involves protolysis of the C–C bond of the paraffin, generating light hydrocarbons C_1, C_2, . . . via nonclassical pentacoordinated carbonium ions (PCI) (*28, 29*).

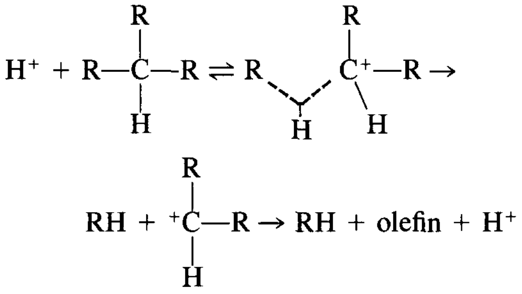

$$H^+ + R-\overset{\displaystyle R}{\underset{\displaystyle H}{C}}-R \rightleftharpoons R\underset{\displaystyle H}{\cdot\cdot\vee\cdot\cdot}\overset{\displaystyle R}{C^+}\!\underset{\displaystyle H}{\diagdown}\!-R \rightarrow$$

$$RH + {}^+\overset{\displaystyle R}{\underset{\displaystyle H}{C}}-R \rightarrow RH + \text{olefin} + H^+$$

The nonclassical ion contains a carbon atom less electron deficient than that in the classical carbenium ion since it is bound by three single bonds and a two-electron, three-center bond.

According to Olah (*26*) "the preferred direction of attack by the proton should not be dogmatically considered always to be the same . . . it will depend on the individual reaction conditions." It was shown that this second mechanism, which is monomolecular, predominates at high temperatures and low pressure (*13, 14, 28*) and is effective particularly for zeolites with high Si/Al ratios.

Whether β-scission or the PCI mechanism is involved, more activation energy is necessary to split a C–C bond at the end of a chain than in the middle, and this energy decreases as the length of the cracked molecule increases. As to the effect of tempera-

TABLE 6

C_3/C_4 Ratio in FCC Cracking[a]

Zeolite	Conversion (%)	C_3/C_4 (volume)
RE-OFF	56.4	1.3
RE-Gmelenite	54.5	1.2
RE-Y	69	0.6
RE-X	55	0.4

[a] Calculated from total C_3 and total C_4 given in Ref. (*20*).

ture on those mechanisms, β-scission should become increasingly important at high temperature compared to the other steps occurring during cracking (*30*). It was also shown that in ZSM-5 and Y the higher production of C_2 as temperature is increased arises because the PCI mechanism is favored over β-scission (*28*). The results in Fig. 8 are in line with this statement.

Considering *n*-heptane cracking, pure β-scission would give a C_3/C_4 ratio of unity in the simplified reaction

$$n\text{-}C_7 \rightarrow C_3 + C_4. \quad (1)$$

Table 3 reports, for all zeolites, values lying between 0.8 and 1.7 (around 1). For *n*-decane cracking the following reactions can occur:

$$\begin{aligned} n\text{-}C_{10} &\xrightarrow{a} C_3 + C_7 \\ n\text{-}C_{10} &\xrightarrow{c} C_4 + C_6 \\ n\text{-}C_{10} &\xrightarrow{e} C_5 + C_5 \quad (2) \\ C_7 &\xrightarrow{b} C_3 + C_4 \\ C_6 &\xrightarrow{d} C_3 + C_3 \end{aligned}$$

According to the relative rates of reactions a to d, it is not possible to calculate C_3/C_4 ratios and then to account for the ratios reported in Table 3 from 1.07 to 3.1. Nevertheless, it turns out that the experimental values are around 2, which could arise by considering only the very simple reactions, a and b. It is well known that polymerization, condensation, and recracking reactions can change the ratios calculated from simple reactions. This may explain the deviations. However, none of these schemes can explain the C_2 production and the changes in the C_2/C_4 ratios observed, parallel to the C_3/C_4 ones. The monomolecular mechanism (PCI) which enables the C–C split at the end of a chain does so.

The most interesting hypothesis to explain selectivity changes observed in the present paper is to consider, as previous authors did for faujasite and ZSM-5 (*13, 28, 29*), that both mechanisms for C–C splitting exist simultaneously in the cracking in zeolites. With any zeolite, for high C_2/C_4 and C_3/C_4 ratios, the PCI mechanism would predominate. Such a situation occurs (i) in small or tortuous channels, (ii) when for a given cage or channel the density of negative charges decreases, (iii) in the presence of polarizing polyvalent cations, and (iv) as the temperature is raised. In contrast, the relative extent of the two mechanisms appears not to be directly related to the following factors: (i) the acid strength in itself, (ii) the density of protons, (iii) for a given cage type the free geometric volume left available to the reactant since coke was deposited during aging and restricting the pore size does not significantly change the C_2/C_4 and C_3/C_4 ratios [Table 2 and Ref. (*8*)]. The distribution of charges in the space surrounding the reactants in the cages can then be considered as the leading parameter. It may be surprising that in solution very strong protons of superacid type are needed to form the pentacoordinated ion, whereas it has been observed that in zeolites acid strength is not an important parameter. Molecules in cages are disturbed by the field and field gradient. This would weaken some C–C bonds which are easily split by protons of even intermediate strength.

The four factors affecting the cracking mechanism can be rationalized by a field gradient effect. Molecules moving in small pores, jumping from one cage to another through small windows, are subject to the strong influence of the wall atoms much more than those in large cavities (Fig. 3). The field gradient, which may vary rapidly within a tenth of a nanometer (*31*), is then high within the volume of a molecule and greatly varies as the moving molecule is close to or far from TO_4 tetrahedra and cations held in configurations depending on each structure topology. In addition, a low density of AlO_4^- tetrahedra in a given zeolite framework also increases the field gradient due to a larger distance between the charges (Table 4).

Polarization of molecules in cavities may create multipole moments as it does for cyclopropane, for instance (*32*). Meanwhile a quadrupole moment makes the molecules dependent on field gradient. In addition, it has been shown than *n*-alkanes such as *n*-decane acquire on adsorption in zeolites a gauche configuration (*33*). Even though little is known of the shape of molecules and of their electron distribution when they are in cages, these examples show that hydrocarbons in zeolites cannot be considered to be the same as in the gas or liquid phases. They are subject to constraints that change their reactivity (*1*) and, as proposed here, may direct the selectivity of the C–C splitting when the field gradient is high.

The increase in the contribution of the PCI mechanism with increasing temperature has been explained by a reduced sorption ability for hydrocarbons and consequently a lower probability for the bimolecular β-scission mechanism (*28*). It is presently suggested that increasing the temperature should favor the perturbing effect of the zeolite on the molecule and then the field gradient–quadrupole interaction. The energy of this interaction also increases with temperature (*31*). As a result an increase in the role of the PCI mechanism is expected.

Accordingly, a relation is observed between the polarization of the molecules, a high field gradient, and high C_3/C_4 ratios associated with the PCI mechanism. Reciprocally, the classical β-scission mechanism would prevail only for nonstrained or slightly electronically or geometrically strained molecules. As the strength of the proton does not seem to interfere directly with the mechanism orientation, it is deduced that it is mainly the electronic and geometric state of the molecule (e.g., C–C bond energies) that directs the mode of cracking (protolysis or β-scission). Let us note that in liquid catalysis, where the molecules should not be disturbed by field gradients, the strength of the proton becomes determining, as shown by Olah (*26, 27*). Why a disturbed molecule will be preferentially attacked by a proton near its end (light product formation) remains an open question.

CONCLUSION

The ratios C_2/C_4 and C_3/C_4 of the products formed in the cracking of alkanes are related to the respective extents of β-scission and pentacoordinated carbonium ion mechanisms. The field gradient should direct the occurrence of the latter mechanisms. In that sense the following points can be outlined: (i) the selectivity ratios are proposed to evaluate the field gradient through the importance of the formation of light products and they could be used as indexes (field gradient selectivity index) to characterize the cracking reaction products; (ii) due to the factors affecting the field gradient these selectivity ratios allow a possible prediction of the formation of light products according to the porosity (pore size and tortuosity), the density of charges, and the polarizing power and density of polyvalent cations; (iii) accordingly, the selectivity could be adjusted by acting on those parameters for all zeolites; (iv) on the reverse side, information may be obtained on one of those three parameters, for instance porosity, if the selectivity ratios and elemental analysis are known; (v) the field gradient selectivity whose origin is energetic in nature may of course exist independently or simultaneously with shape selectivity; and (vi) the present conclusions are valid for branched alkanes, isooctane being an example (*8*), at least for zeolites whose pore sizes allow the entry of these molecules.

ACKNOWLEDGMENT

The authors thank the referees for valuable suggestions.

REFERENCES

1. Rabo, J. A., Pickert, P. E., Stamires, D. N., and Boyle, J. E., *in* "Proceedings, International Congress on Catalysis, 2nd (Paris, 1960)," p. 2055. Technip. Paris, 1961.

2. Pickert, P. E., Rabo, J. A., Dempsey, E., Schomaker, V., *in* "Proceedings, International Congress on Catalysis, 3rd (Amsterdam, 1964)," p. 714. North-Holland, Amsterdam, 1965.
3. Weisz, P. B., *in* "Catalysis" (T. Seiyama and K. Tanabe, Eds.), Part A, p. 3. Elsevier, Amsterdam, 1981.
4. Patton, R. L., Flanigen, E. M., Dowell, L. G., and Passoja, D. E., *Amer. Chem. Soc. Symp. Ser.* **40,** 64 (1977).
5. Jarman, R. H., and Melchior, M. T., *J. Chem. Soc. Chem. Commun.,* 414 (1984).
6. Fraissard, J., Ito, I., Springuel-Huet, M., and Demarquay, J., *in* "Proceedings, 7th International Zeolite Conference, 1986" (Y. Murakami, A. Iijima, and J. W. Ward, Eds.), p. 393. Kodansha, Elsevier, Tokyo, 1986.
7. Mirodatos, C., and Barthomeuf, D., *J. Catal.* **57,** 136 (1979).
8. Mirodatos, C., and Barthomeuf, D., *J. Catal.* **93,** 246 (1985).
9. Barthomeuf, D., and Beaumont, R., *J. Catal.* **30,** 288 (1973).
10. Skeels, G. W., and Breck, D. W., *in* Proceedings, 6th International Zeolite Conference (D. Olson and A. Bisio, Eds.), p. 87. Butterworths, London, 1984.
11. Barrer, R. M., and Harding, D. A., *Sep. Sci.* **9,** 195 (1974).
12. Mirodatos, C., Abou-Kais, A., Védrine, J. C., and Barthomeuf, D., *J. Chem. Soc. Faraday Trans. 1* **74,** 1786 (1978).
13. Giannetto, G., Sansare, S., and Guisnet, M., *J. Chem. Soc. Chem. Commun.,* 1302 (1986).
14. Mirodatos, C., and Barthomeuf, D., "AIChE Spring Meeting, Zeolite Catal. Symposium, 1986," Paper 46b (microfilm).
15. Mirodatos, C., Biloul, A., and Barthomeuf, D., *J. Chem. Soc. Chem. Commun.,* 149 (1987).
16. Dempsey, E., *in* "Molecular Sieves," p. 293. Society of Chemical Industry, London, 1968.
17. Pine, L. A., Maher, P. J., and Wachter, W. A., *J. Catal.* **85,** 466 (1984).
18. Mirodatos, C., and Barthomeuf, D., *J. Chem. Soc. Chem. Commun.,* 39 (1981).
19. Gorring, R. L., *J. Catal.* **31,** 13 (1973).
20. Vaughan, D. E. W., *in* "Properties and Applications of Zeolites" (R. P. Townsend, Ed.), p. 294. Chem. Soc., London, 1980.
21. Mahtout, T., Thèse, Rueil-Malmaison, 1985.
22. Frilette, V. J., Weisz, P. B., and Golden, R. L., *J. Catal.* **1,** 301 (1962).
23. Rabo, J. A., and Poutsma, M. L., *Adv. Chem. Ser.* **102,** 284 (1971).
24. McVicker, G. B., Kramer, G. M., and Ziemak, J. J., *J. Catal.* **83,** 286 (1983).
25. Venuto, P. B., and Habib, E. T., Jr., "Fluid Catalytic Cracking with Zeolite Catalysts," p. 103. Dekker, New York, 1979.
26. Olah, G. A., *J. Amer. Chem. Soc.* **94,** 808 (1972).
27. Olah, G. A., Prakash, G. K. S., and Sommer, J., *in* "Superacids," p. 244. Wiley, New York, 1985.
28. Haag, W. O., and Dessau, R. M., *in* "Proceedings, 8th International Congress on Catalysis, (Berlin, 1984)," Vol. II, p. 305. Verlag Chemie, Weinheim, 1984.
29. Corma, A., Monton, J. B., and Orchilles, A. V., *Appl. Catal.* **16,** 59 (1985); *Ind. Eng. Chem. Prod. Res. Div.* **23,** 404 (1984).
30. Poutsma, M. L., *in* "Zeolite Chemistry and Catalysis" (J. A. Rabo Ed.), Vol. 171, p. 529. Amer. Chem. Soc., Washington, DC, 1976.
31. Barrer, R. M., *in* "Zeolites and Clay Minerals," p. 183. Academic Press, New York, 1978.
32. Kiselev, A. V., *in* "Proceedings, 5th International Zeolite Conference" (L. V. Rees, Ed.), p. 400. Heyden, London, 1980.
33. Fiedler, K. Lohse, V., Sauer, J., Stach, H., Thamm, H., and Schirmer, W., *in* "Proceedings, Fifth International Zeolite Conference" (L. V. Rees, Ed.), p. 490. Heyden, London, 1980.